



This is a repository copy of *Experimentation and modelling of near field explosions*.

White Rose Research Online URL for this paper:  
<http://eprints.whiterose.ac.uk/105009/>

Version: Accepted Version

---

**Proceedings Paper:**

Fuller, B., Rigby, S.E., Tyas, A. et al. (4 more authors) (2016) Experimentation and modelling of near field explosions. In: Proceedings of the 24th Military Aspects of Blast and Shock. 24th Military Aspects of Blast and Shock, 19-23 Sep 2016, Halifax, Nova Scotia, Canada. MABS .

---

**Reuse**

Unless indicated otherwise, fulltext items are protected by copyright with all rights reserved. The copyright exception in section 29 of the Copyright, Designs and Patents Act 1988 allows the making of a single copy solely for the purpose of non-commercial research or private study within the limits of fair dealing. The publisher or other rights-holder may allow further reproduction and re-use of this version - refer to the White Rose Research Online record for this item. Where records identify the publisher as the copyright holder, users can verify any specific terms of use on the publisher's website.

**Takedown**

If you consider content in White Rose Research Online to be in breach of UK law, please notify us by emailing [eprints@whiterose.ac.uk](mailto:eprints@whiterose.ac.uk) including the URL of the record and the reason for the withdrawal request.



[eprints@whiterose.ac.uk](mailto:eprints@whiterose.ac.uk)  
<https://eprints.whiterose.ac.uk/>

# EXPERIMENTATION AND MODELLING OF NEAR FIELD EXPLOSIONS

B Fuller<sup>1</sup>, SE Rigby<sup>1</sup>, A Tyas<sup>1,2</sup>, SD Clarke<sup>1</sup>, JA Warren<sup>1,2</sup>, J Reay<sup>2</sup>, M Gant<sup>3</sup>, I Elgy<sup>3</sup>

<sup>1</sup>*University of Sheffield, Department of Civil & Structural Engineering, Sir Frederick Mappin Building, Mappin Street, Sheffield, S1 3JD, UK;*

<sup>2</sup>*Blastech Ltd., The BioIncubator, 40 Leavygreave Road, Sheffield, S3 7RD, UK;*

<sup>3</sup>*Defence Science and Technology Laboratory (Dstl), Porton Down, Salisbury, Wiltshire, SP4 0JQ, UK.*

## ABSTRACT

Repeatable experimental results and numerical work has shown that using the Jones-Wilkins-Lee (JWL) equation of state (EOS) will give very accurate results of peak pressures and impulse delivered to a rigid target at large scaled distances. However, recent experiments/numerical modelling at small scaled distances show that the JWL will over-predict peak pressures and impulse due to the assumption of (near) instantaneous energy release from detonation. The results of this experimental/numerical study are presented herein. In the experimental work PE4 spheres at two different scaled distances have been tested using an array of Hopkinson Pressure Bars (HPB) at specific points on a rigid target to measure the local pressure-time histories. From the HPB measurements, it appears that below certain scaled distances there are chemical-physical mechanisms that do not have sufficient time to contribute to the energy driving the loading mechanisms, explaining the over-prediction of the JWL. Importantly though, the experimental results show that at very small scaled distances ( $0.172 \text{ m/kg}^{1/3}$ ) the test to test percentage variation is very low (5.1%); whilst at larger scaled distances ( $0.819 \text{ m/kg}^{1/3}$ ) it is much higher (23.1%). This paper presents a model which describes the process by which experimental results move from repeatable to variable to repeatable as scaled distance increases from the extreme near field to far field.

## INTRODUCTION

Accurate, repeatable experimental data is not often available for a robust assessment of modeling approaches for near field blast events. Rigid or semi-rigid targets in the near field will interact with expanding detonation products and affect the physical processes taking place therein. Therefore, using data such as arrival time and incident pressures from non-disruptive measurement systems may not be suitable for validating a modelling approach where the target is a reflecting and disruptive surface.

The calculation of JWL equations of state involves fixing  $E_0$ , the total energy density from calorimetry, and adjusting the EOS parameters to fit. [1] [2] It is hypothesized in this paper that the total quantity of  $E_0$  is not released as a result of detonation, but that a substantial amount of energy is only released as a result of the secondary combustion (afterburn) of the detonation products. These secondary reactions can only occur as the expanding detonation products encounter fresh oxygen, which takes significant time compared to detonation process. When using the JWL EOS all the energy available to the system is released at detonation. This paper presents experimental work measuring the reflected pressures generated as a result of the detonation of PE4 spheres in close proximity to a large nominally rigid target as well as a numerical study using LS-DYNA.

## EXPERIMENTAL WORK

### Setup

The experimental methodology used in this work has been reported in detail in [3] however brief details are presented here for the reader's convenience. The testing rig consists of two reinforced concrete reaction frames, a rigid steel target plate, load cells and an array of HPBs. Figure 1 and Figure 2 give details of important dimensions and the overall layout of the rig. The rigid target plate is slung under the reaction frames bearing up against the 50 mm thick steel plates cast into both concrete frames. Each HPB passes through the rigid target plate in a slightly oversized hole, such that the loaded faces of the HPBs are flush with the face of the target plate. The HPBs are furnished with perimeter strain gauges mounted in pairs on opposite sides of the bar. This arrangement captures axial strain on the bar surface; while also automatically compensating for stresses due to bending, using the arrangement of the circuit. Blast events load the face of a HPB causing a stress pulse to travel down the bar straining the gauge material as it passes. This strain causes a change in voltage with time across the strain gauge arrangement. The data is recorded using an oscilloscope with sufficient voltage resolution and sampling rate to accurately capture the expected changes in voltage due to the mechanical strain of the gauges. In this way, for every discrete HPB location in the array, the pressure-time history on the loaded face of the bar can be calculated from the voltage-time history.

The spherical charges were supported under the centre of the target plate on a taut layer of thin glass-fibre fabric (density  $25\text{g/m}^2$ ). This allowed accurate support and alignment of the charge with minimal difference to the "free air" event.

Details of the arrangement of the tests are given in the table below.

Table 1: Charge details of the 6 tests

Test Number	Explosive Material	Charge Mass (grams)	Standoff to Charge Centre (mm)	Scaled Distance ( $\text{m/kg}^{1/3}$ )
1	PE4	100	80	0.172
2	PE4	100	80	0.172
3	PE4	100	80	0.172
4	PE4	100	380	0.819
5	PE4	100	380	0.819
6	PE4	100	380	0.819

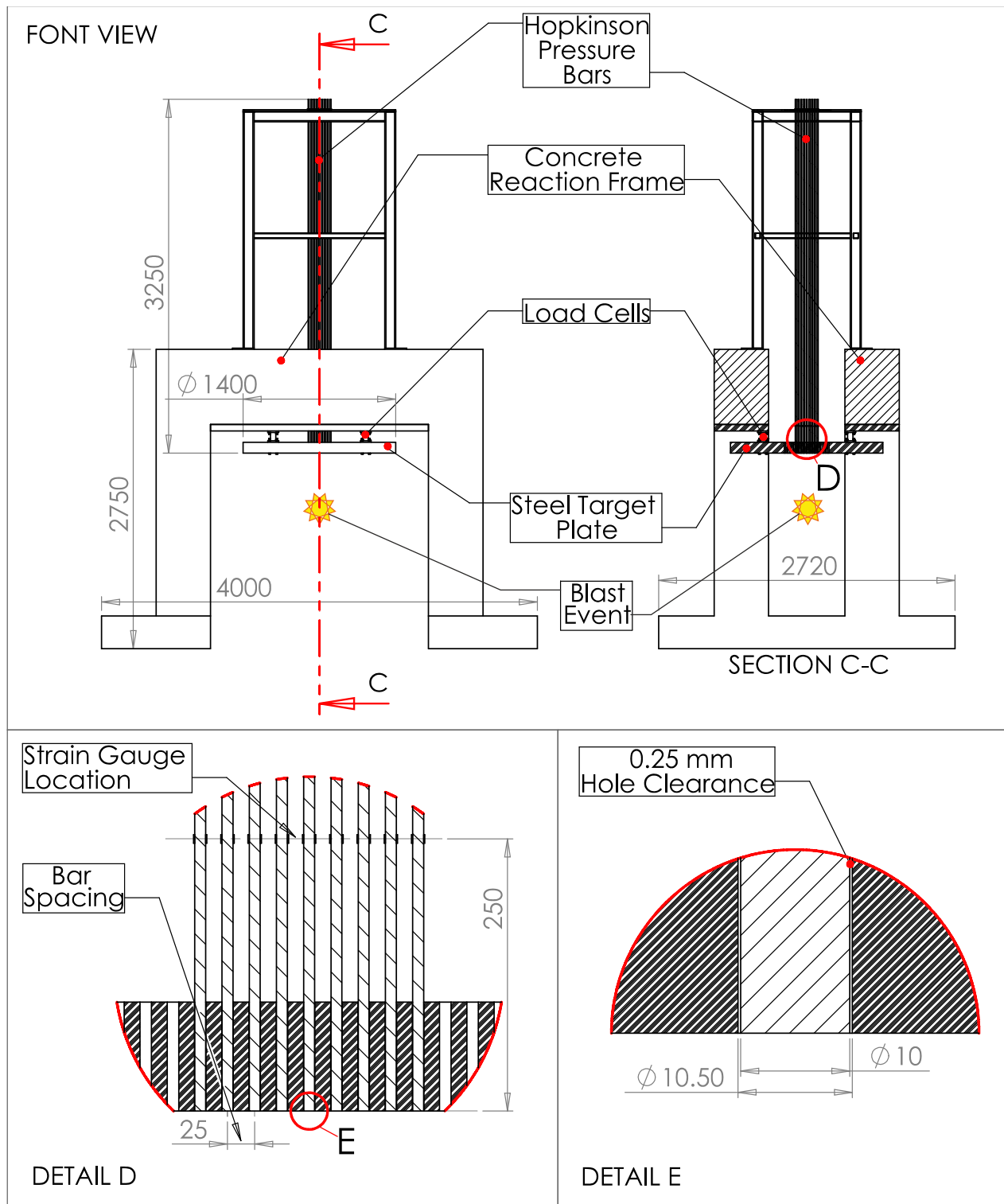


Figure 1: Testing rig details (units: mm)

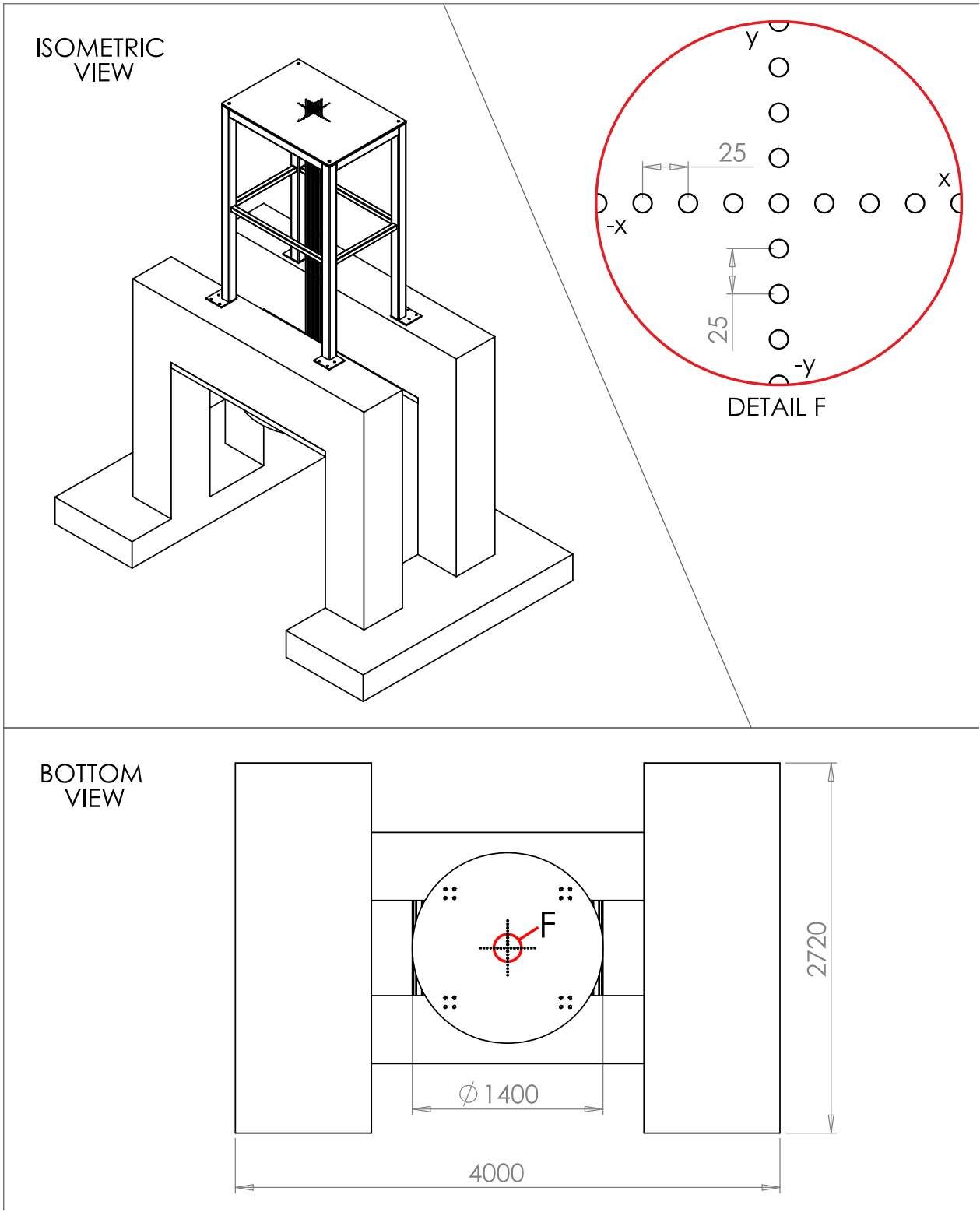


Figure 2: Testing rig details (units: mm)

## Results

The figures in this section aim to present the results of the experimental work using a range of perspectives; from spatially discrete pressure-time histories to total spatially integrated impulse. Figure 3 and Figure 4 are samples of the pressure-time histories recorded at each bar location for the 80 mm and 380 mm stand-off tests respectively. Figure 5 and Figure 6 are the pressure-time histories from figure 3 and Figure 4 integrated in time for each bar location showing the accumulation of specific impulse with time.

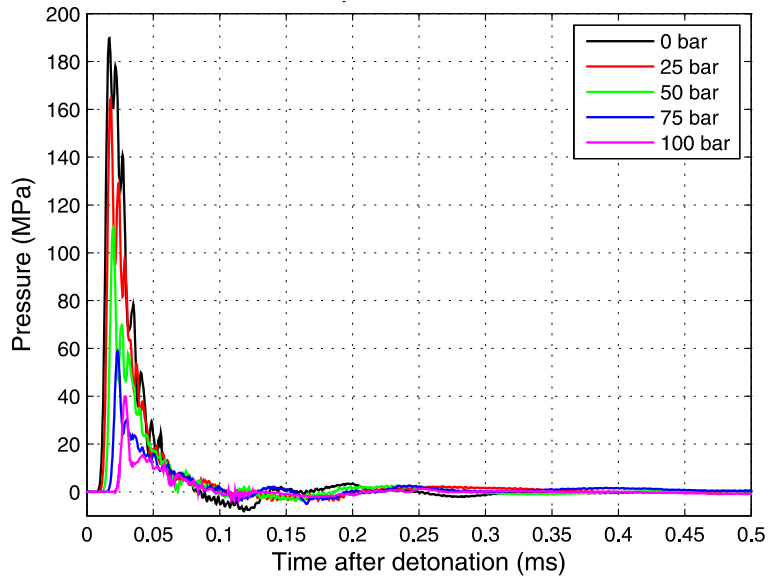


Figure 3 : Example pressure-time history from test 3, -y radial ordinate

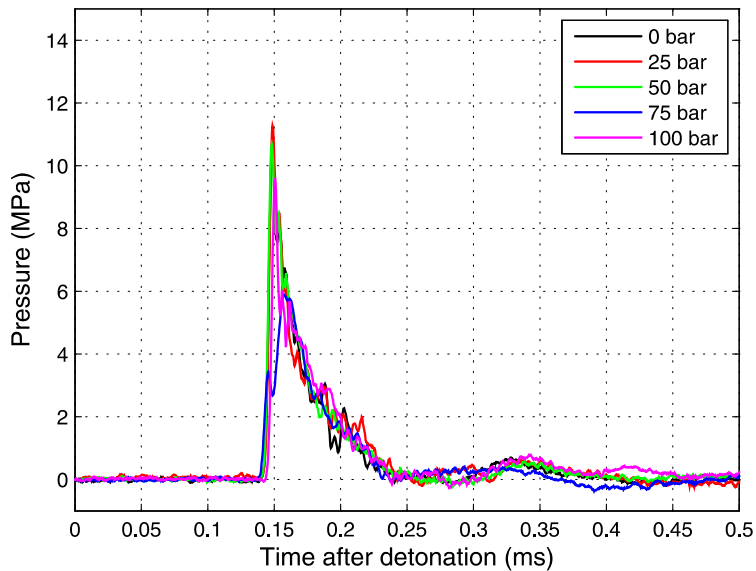


Figure 4 : Example pressure-time history from test 4, -y radial ordinate

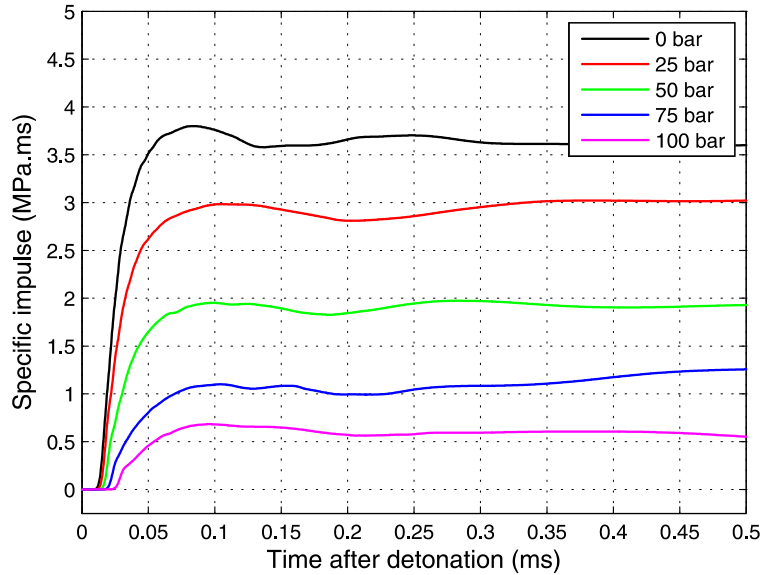


Figure 5 : Example specific impulse history from test 3, -y radial ordinate

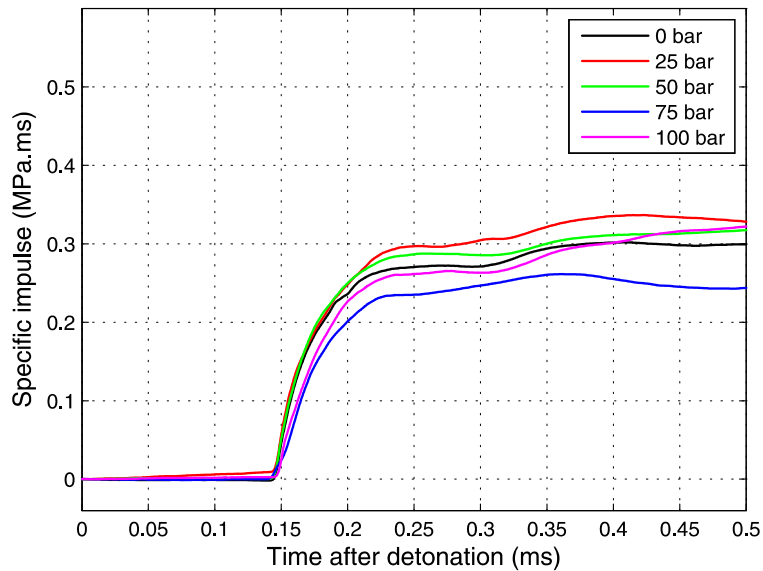


Figure 6 : Example specific impulse history from test 4, -y radial ordinate

The peak pressure at each bar location has been determined and the values from bar locations with the same radial offset have been averaged together as shown in Figure 7; the same has been done for peak specific impulse as shown in Figure 8. Finally, Figure 9 shows the total impulse over a 100 mm radius; which has been determined for each test by interpolating, and integrating over 200 discrete radial bands of area.

Tests 4-6 are much closer to a plane wave scenario than tests 1-3 where the decay in pressure and impulse with increasing radial distance is almost an order of magnitude in 100 mm. The most evident trend from the experimental results is the difference in the repeatability of the pressure-

time histories at any radial offset when comparing tests 1-3 to tests 4-6. Tests 1-3 show remarkably repeatable results for every radial offset of peak pressure with a maximum variation of 5.1% from the median over the 3 tests. Whilst tests 4-6 show a much larger percentage of variation at each radial offset with a maximum variation of 23.1% from the median over the 3 tests. Figure 10 illustrates an explanation which considers the physical phenomena taking place as the source of variation. Photo (a) shows a 100g sphere of PE4 just after the detonation products have begun to expand outwards and the surface of the expanding fireball is relatively uniform. Photo (d) shows this same event  $\sim 87\mu\text{sec}$  later where the detonation products have expanded  $\sim 75$  times by volume; crucially though, it can be seen that large instabilities have developed on the surface of the detonation products which is also still driving the shock front which has not yet detached from the detonation products. It is clear that the turbulent growth of these instabilities, on the surface of the expanding detonation products, is the most likely source of increased variation in the discrete pressure-time histories for tests 4-6.

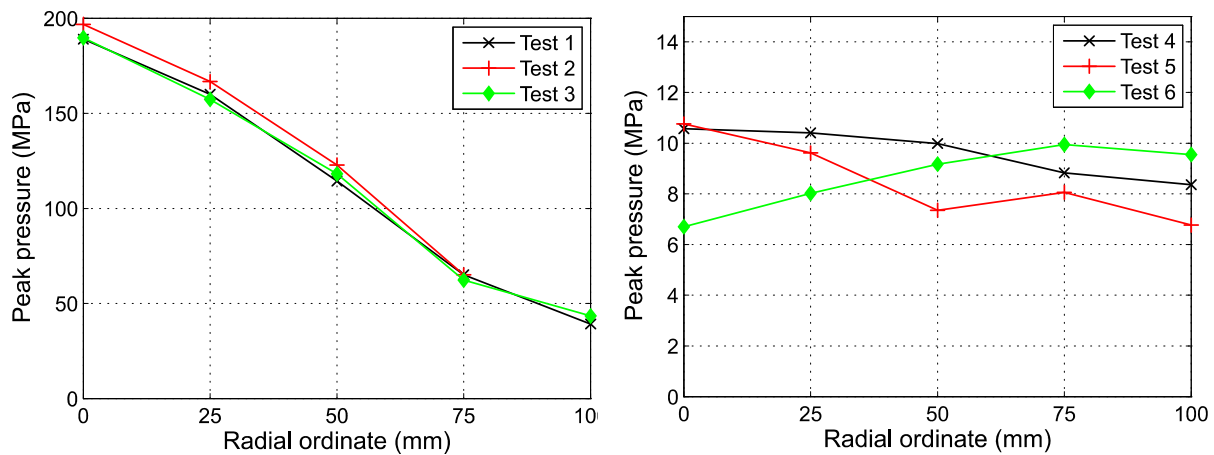


Figure 7: Average of peak pressures at each radial offset for tests 1-6

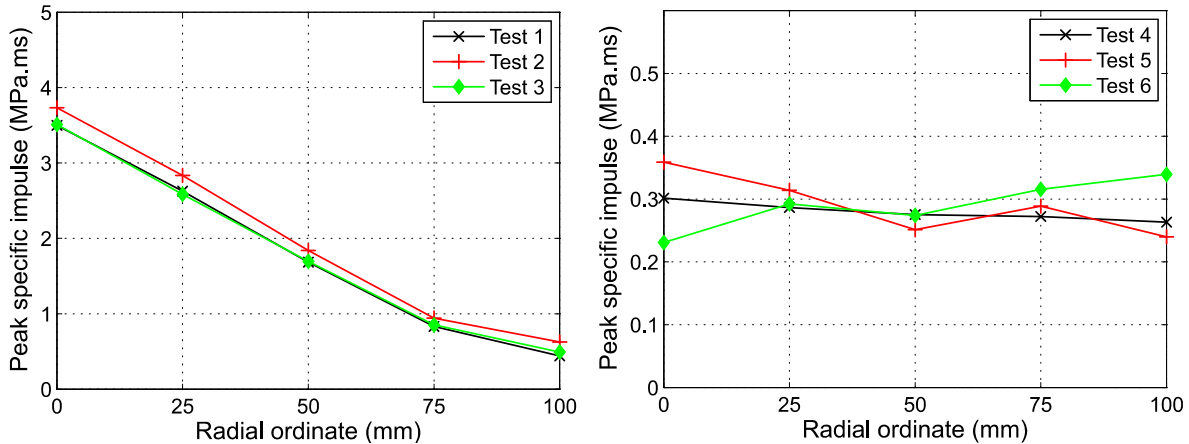


Figure 8: Average of peak specific impulse at each radial offset for tests 1-6



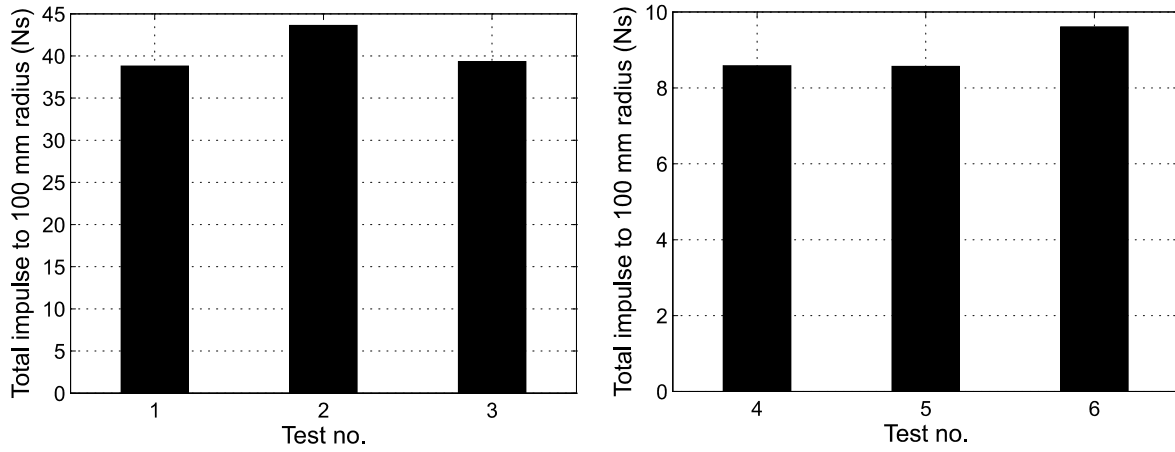


Figure 9: Total impulse integrated over 100 mm radius for tests 1-6

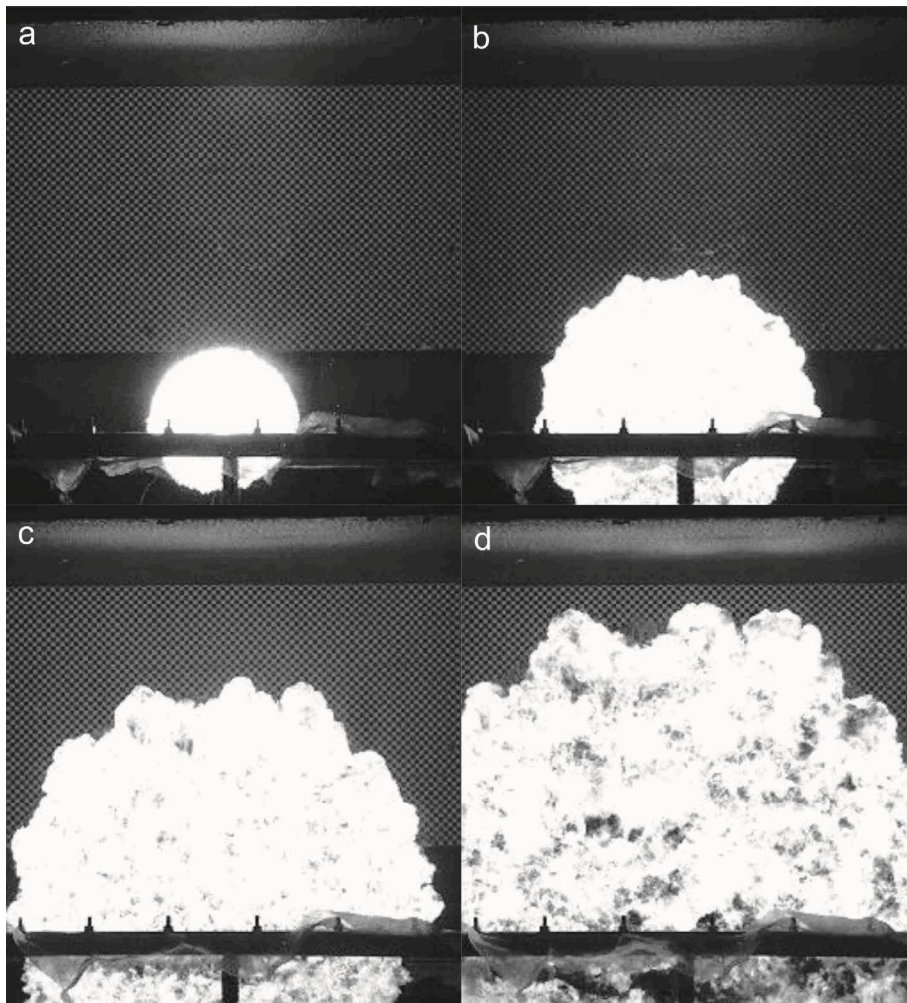


Figure 10: 100g sphere PE4 at four times after detonation: (a)  $\sim 12\mu\text{sec}$ , (b)  $\sim 31\mu\text{sec}$ , (c)  $\sim 62\mu\text{sec}$ , (d)  $\sim 99\mu\text{sec}$

## MODELLING WORK

### Setup

The explicit numerical code LS-DYNA [4] was used to perform an Arbitrary-Lagrangian-Eulerian (ALE) analyses of the two scenarios detailed in the experimental setup. Because the test arrangement was suitable, these analyses were completed in an axi-symmetric domain about the axis of the central HPB. The mesh was generated as a regular square grid large enough to avoid any complications as a result of material interaction with the model boundaries. Although a radial mesh symmetric about the charge centre and the central HPB axis was used to detonate and expand the explosive material to the point just before any interaction with the rigid boundary; at which point it was remapped onto the rectangular mesh. This was done to avoid the advection errors associated with material transportation at 45° to a square mesh. A mesh sensitivity analysis was performed. \*BOUNDARY\_SPC\_NODE was used to simulate the rigid boundary of the target face in the experimental rig. Numerical information in the model was recorded for the locations of the experimental pressure bars using \*DATABASE\_TRACER. Figure 11 shows the basic layout of the ALE models. Table 2 gives details of the EOS and material models used in the analyses.[5]

Table 2: Material model and equation of state parameters for PE4 and air (SI units)

	MAT_HIGH_EXPLOSIVE_BURN							
	$\rho_0$	$D$	$PCJ$					
PE4	1601	8193	2.80E10					
	EOS_JWL							
	$A$	$B$	$R_1$	$R_2$	$\omega$	$E_0$		
	609.77E9	12.95E9	4.50	1.40	0.25	9.0E9		
	MAT_NULL							
	$\rho_0$							
Air	1.225							
	EOS_LINEAR_POLYNOMIAL							
	$C_0$	$C_1$	$C_2$	$C_3$	$C_4$	$C_5$	$C_6$	$E_0$
	0.0	0.0	0.0	0.0	0.4	0.4	0.0	253.4E3

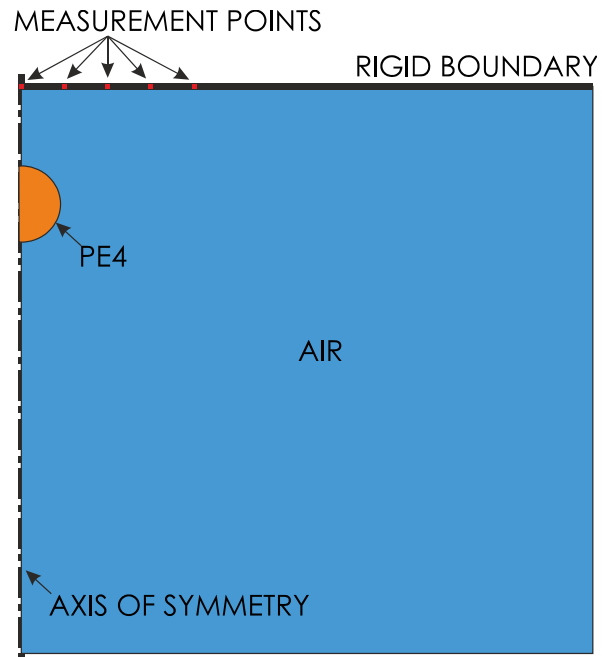


Figure 11: ALE model example schematic

## Modelling results including comparison with experimental tests

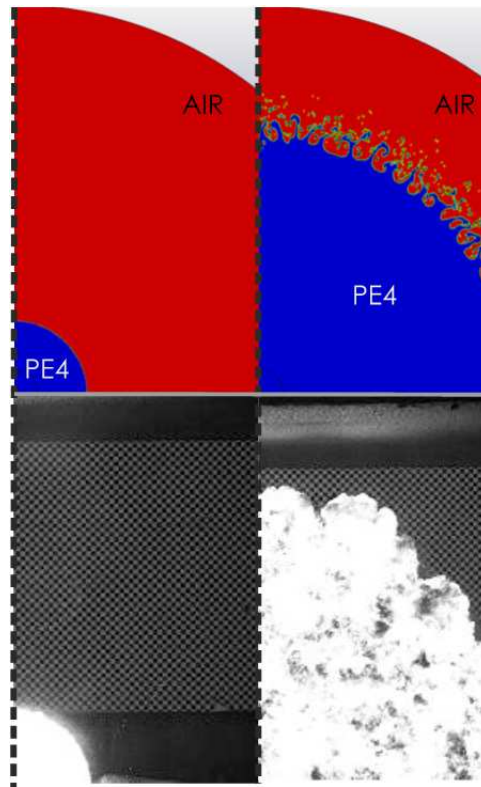


Figure 12: Modelling vs experimental detonation products expansion and instabilities at  $\sim 12\mu\text{sec}$  &  $\sim 99\mu\text{sec}$

The pressure-time histories extracted from the model for the points corresponding to the experimental HPBs were applied to a numerical HPB in LS-DYNA and the resulting stress-time histories at 250 mm from the loaded face (the same as the experiments) of the bar were predicted. It is generally accepted that LS-DYNA numerical models are able to capture the effects of dispersion on the strain signals in the experimental HPBs. In this way the ALE modelling results can be post processed to allow for a more valid comparison with the experimental data; although both the raw outputs and the post processed outputs will be shown for completeness.

With respect to the development of instabilities in the detonation products with volumetric expansion Figure 12 provides a qualitative comparison on this phenomenon between the experimental HSV and the modelling results. It is worth noting that the modelling does not consider secondary combustion of the detonation products as a result of mixing with the air; which will certainly be a significant factor in the development and effects of this turbulent zone. It is likely that the instabilities seen in the modelling are Raleigh Taylor instabilities that are preserved by this modelling technique.

It can be seen in Figure 13 and Figure 14 that the ALE modelling approach used gives reasonably accurate results for both configurations. The overall shape and amplitude of the pressure signal is much closer to the experimental average in tests 4-6. Also, the post processed model output for tests 4-6 show minimal changes as a result of dispersion; this is in direct contrast to the post processed output for tests 1-3. The post processed model output for tests 1-3 shows significant

dispersion effects compared to the experimental average suggesting that the loading pulse in the experiments would have contained less high frequency content (sharp features) than the raw model results.

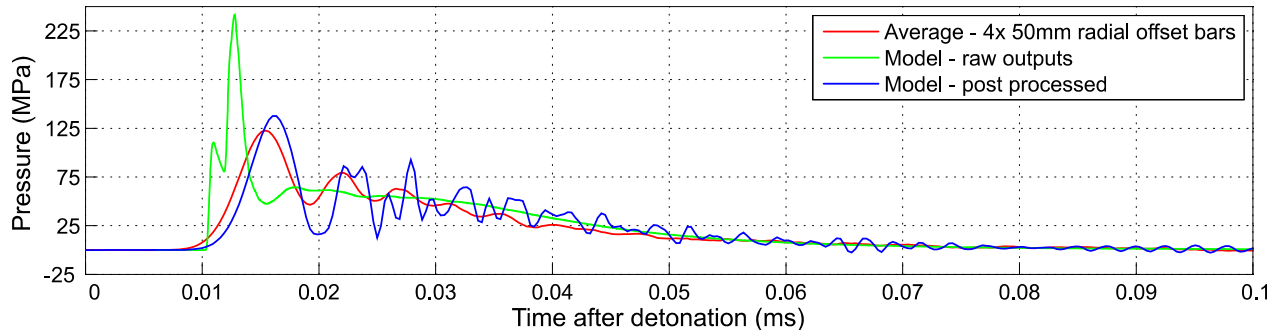


Figure 13: Sample comparison of experimental measurements vs model results – test 2

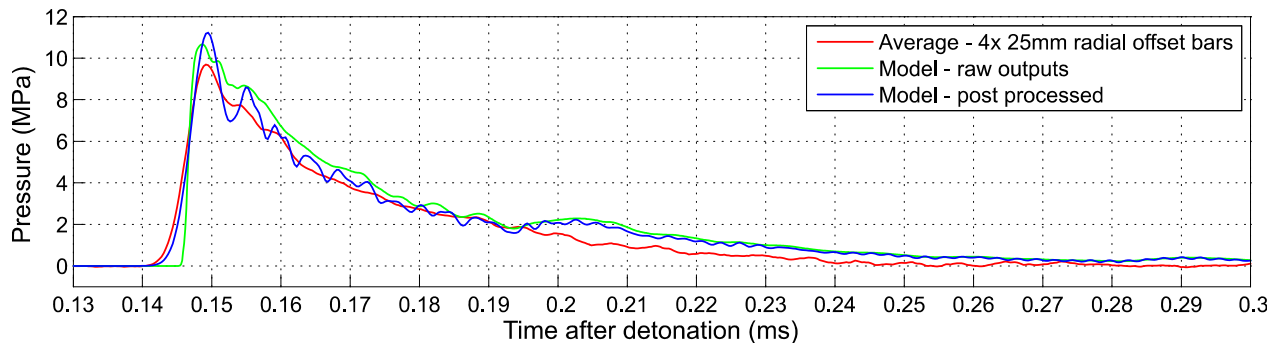


Figure 14: Sample comparison of experimental measurements vs model results – test 4

The 4 subsequent tables provide a detailed comparison the average experimental results and the model results at each bar location for both peak pressure and peak specific impulse, considering both the raw model outputs and the post processed outputs. The model generally over-predicts pressure and impulse in all tests as seen in Tables 3 & 4.

Table 3: Comparison of numerical modelling results with averaged experimental results - 80 mm standoff, tests 1-3

Peak pressure (MPa)					
Radial offset (mm)	Experimental average (3 tests)	Model	Error	Model – post processed	Error
0	192	577	+200%	257	+33%
25	161	479	+197%	219	+36%
50	118	240	+103%	137	+16%
75	64	120	+87%	77	+20%
100	47	74	+57%	44	-6%

Table 4: Comparison of numerical modelling results with averaged experimental results - 380 mm standoff, tests 4-6

Peak pressure (MPa)					
Radial offset (mm)	Experimental average (3 tests)	Model	Error	Model – post processed	Error
0	9.3	10.7	+15%	11.4	+22%
25	9.3	10.6	+14%	11.2	+20%
50	9.0	11.8	+31%	10.8	+20%
75	8.9	10.2	+15%	10.2	+15%
100	8.2	9.3	+13%	9.7	+18%

Table 5: Comparison of numerical modelling results with averaged experimental results - 80 mm standoff, tests 1-3

Peak specific impulse (MPa.ms)					
Radial offset (mm)	Experimental average (3 tests)	Model	Error	Model – post processed	Error
0	3580	4170	+16%	3863	+8%
25	2682	3555	+33%	3283	+22%
50	1732	2310	+33%	2131	+23%
75	875	1380	+57%	1273	+45%
100	519	851	+63%	778	+50%

Table 6: Comparison of numerical modelling results with averaged experimental results - 380 mm standoff, tests 4-6

Peak specific impulse (MPa.ms)					
Radial offset (mm)	Experimental average (3 tests)	Model	Error	Model – post processed	Error
0	297	363	+22%	337	+13%
25	298	349	+17%	324	+9%
50	268	338	+26%	314	+17%
75	292	326	+12%	303	+4%
100	280	314	+12%	292	+4%

Because the percentage of error between model and experimental results for specific impulse changes significantly with increasing radial offset for tests 1-3, the modeling results (post processed) have been integrated over the 100 mm radius and compiled together with the

experimental results for a direct global comparison in Figure 15. This comparison shows that even though the magnitude of the specific impulse farther from the centre of the target may be low, an error can have significant effects on the total global impulse .

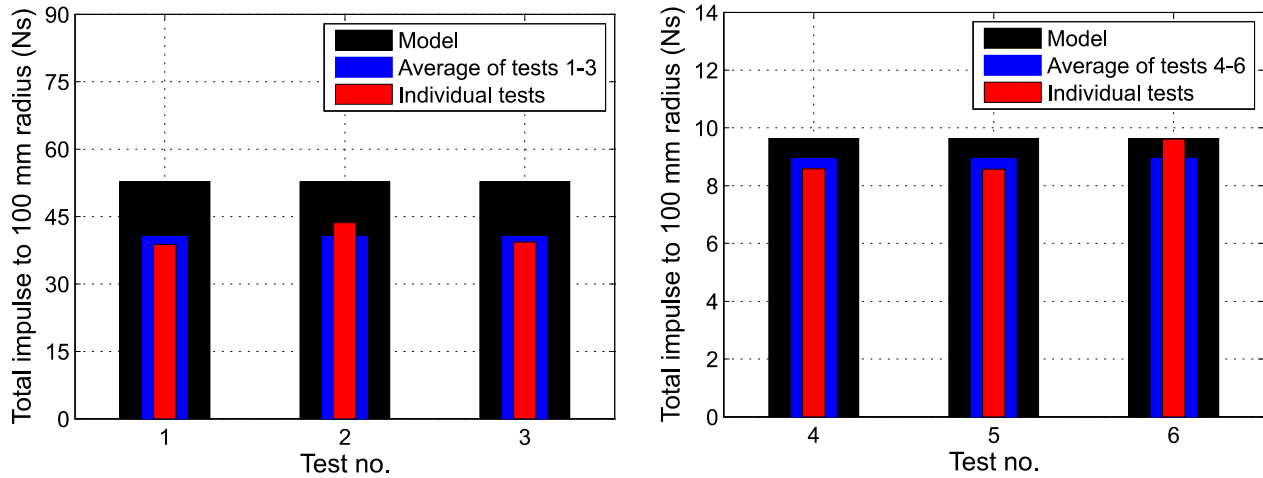


Figure 15: Total impulse integrated over 100 mm radius for tests 1-6 with modeling results and test averages

## DISCUSSION/CONCLUSIONS

First, an interrogation of the HSV and the experimental measurements show that the relative magnitude of surface instabilities increases as the detonation products expand outward (Figure 10). Meaning that for any discrete point of interest on a rigid target the loading will be much more repeatable at smaller scaled distances. However, this criterion for repeatability will only apply to the range of scaled distances where detonation products are still affecting the shock front and a significant proportion of the loading is due to the reflection of the detonation products. That is, in the far field where targets are only affected by the detached shock front the repeatability of results will be higher than in this intermediate range. Repeatable results in the far field have been demonstrated in Rigby et al. [6]. Interestingly, the amount of test to test variation seen in the global impulse results is almost the same between tests 1-3 and 4-6; meaning that even though local pressure time histories may vary test to test, the global loading does not.

Second, the over prediction of local peak pressures, specific impulses and global impulse increases as scaled distance decreases for the LS-DYNA ALE numerical modelling formulation and the JWL equation of state. With respect to raw model outputs in this paper, peak pressure for a scaled distance of  $0.172\text{m/kg}^{1/3}$  is over predicted by as much as 200%, whilst for a scaled distance of  $0.819\text{ m/kg}^{1/3}$  is only over predicted by 15%. Also, peak specific impulse for the smaller scaled distance is over predicted by as much as 63%, whilst for the larger scaled distance is only over predicted by 22%. The most convincing evidence of the over prediction is the global impulse results. For the smaller scaled distance the average global impulse over prediction is 30% and only 8% for the larger scaled distance. In Rigby et al. [6] all the scenarios considered have a scaled distance greater than  $6\text{ m/kg}^{1/3}$  and it is reported that the same ALE LS-DYNA modelling approach will actually under predict both peak pressures and peak specific impulse.

Finally, the results and comparisons presented in this paper show that repeatable experimental measurements of reflected pressure are possible at very small scaled distances, that turbulent instabilities grow with the expansion of the detonation products and that the JWL EOS for PE4 will significantly over predict pressure and impulse in the extreme near field. These findings are in keeping with the hypothesis that the JWL EOS releases the energy associated with secondary combustion upon detonation; rather than over a timescale as a result of mixing with free oxygen in the air.

## REFERENCES

- [1] J. Sanchidrian, R. Castedo, L. Lopez, P. Segarra, A. Santo., 2015, Determination of the JWL Constants for ANFO and Emulsion Explosives from Cylinder Test Data, *Universidad Politecnica*, 12(2), 177-194
- [2] C. Mader, 2008, *Numerical Modeling of Explosives and Propellants*, London, CRC Press
- [3] S.E. Rigby, A. Tyas, S.D. Clarke, S.D. Fay, J. Reay, J.A. Warren, M. Gant, I. Elgy, 2015, Observations from Preliminary Experiments on Spatial and Temporal Pressure Measurements from Near-Field Free Air Explosions, *International Journal of Protective Structures*, 6(2)
- [4] J.O. Hallquist, 2006, *LS-DYNA theory manual*, Livermore Software Technology Corporation
- [5] B.M. Dobratz, P.C. Crawford, 1985, *LLNL explosives handbook*, University of California
- [6] S.E. Rigby, A. Tyas, T. Bennett, S.D. Fay, S.D. Clarke, J.A. Warren, 2014, A Numerical Investigation of Blast Loading and Clearing on Small Targets, *International Journal of Protective Structures*, 5(3)